

## Multipole mixing ratios in $^{77}\text{Se}$ from $\gamma\gamma$ directional correlations following 56-h $^{77}\text{Br}$ decay

Robert A. Braga and Demetrios G. Sarantites

Chemistry Department, Washington University, St. Louis, Missouri 63130\*

(Received 20 September 1973)

The decay properties of the levels in  $^{77}\text{Se}$  were investigated following the decay of 56-h  $^{77}\text{Br}$ . Singles  $\gamma$ -ray energy and intensity measurements were obtained with a 42-cm<sup>3</sup> high-resolution Ge(Li)  $\gamma$ -ray detector in an anti-Compton arrangement employing a large NaI(Tl) annular detector. Extensive  $\gamma\gamma$ -coincidence and directional-correlation measurements were obtained with two large Ge(Li) detectors. An improved decay scheme was constructed. From  $\gamma\gamma$  correlation measurements, deduced  $\log ft$  values, and internal-conversion coefficients, the  $J^\pi$  values in parentheses for the following levels in keV were confirmed: g.s. ( $\frac{1}{2}^-$ ), 161.83 ( $\frac{1}{2}^+$ ), 238.98 ( $\frac{3}{2}^-$ ), 249.65 ( $\frac{3}{2}^-$ ), 439.42 ( $\frac{3}{2}^-$ ), 520.59 ( $\frac{3}{2}^-$ ), 817.78 ( $\frac{1}{2}^-$ ), and 1005.08 ( $\frac{3}{2}^-$ ); and further  $J^\pi$  assignments in parentheses for the following levels are proposed: 300.78 ( $\frac{5}{2}^+$ ), 580.90 ( $\frac{5}{2}^+$ ), 679.7 ( $\frac{5}{2}^+$ ), 824.35 ( $\frac{3}{2}^-$ ,  $\frac{5}{2}^-$ ), 911.40 ( $\frac{3}{2}^+$ ), 1186.55 ( $\frac{3}{2}^-$ ), and 1230.62 ( $\frac{3}{2}^+$ ,  $\frac{5}{2}^-$ ). With the 249.77- and 439.47-keV transitions assumed to be pure  $E2$ , the mixing ratio  $\delta(M2/E1) = -0.09 \pm 0.05$  was obtained for the 87.59-keV transition, while the  $\delta(E2/M1)$  mixing ratios obtained were: 200.40 keV,  $0.00 \pm 0.09$ ; 238.98 keV,  $0.13 \pm 0.04$ ; 270.83 keV,  $0.30^{+0.05}_{-0.06}$ ; 281.65 keV,  $-0.12^{+0.03}_{-0.04}$ ; 297.23 keV,  $0.17 \pm 0.03$  or  $-2.7 \pm 0.2$ ; 303.76 keV,  $-0.44^{+0.05}_{-0.16}$  or  $0.09^{+0.05}_{-0.04}$ ; 384.99 keV,  $-0.23^{+0.07}_{-0.05}$ ; 484.57 keV,  $-0.27^{+0.04}_{-0.03}$ ; 520.69 keV,  $0.17^{+0.06}_{-0.07}$ ; 574.64 keV,  $0.23 \pm 0.06$  for  $\frac{3}{2}^- \rightarrow \frac{5}{2}^-$  or  $-0.31^{+0.07}_{-0.08}$  for  $\frac{5}{2}^- \rightarrow \frac{5}{2}^-$ ; 578.91 keV,  $0.16^{+0.03}_{-0.04}$  or  $-2.6^{+0.2}_{-0.3}$ ; and 755.35 keV,  $0.31^{+0.09}_{-0.08}$ . From these multipole mixing ratios, present branching ratios and previously measured lifetimes improved and new values of reduced transition probabilities were calculated for the transitions at 87.59, 200.40, 238.98, 249.77, 270.83, 277.47, 281.65, 439.47, and 520.69 keV. The results of this study are compared with previous work and the structure of the lower levels in  $^{77}\text{Se}$  is discussed in terms of recent theoretical models for nuclear structure.

[ RADIOACTIVITY  $^{77}\text{Br}$ ,  $^{75}\text{As}(\alpha, 2n)$  at 22 MeV, measured  $E_\gamma$ ,  $I_\gamma$ ,  $\gamma\gamma$ ,  $\gamma\gamma(\theta)$ ;  
deduced  $^{77}\text{Se}$  levels,  $\log ft$ ,  $J$ ,  $\pi$ ,  $\delta(E2/M1)$ ,  $B(E2)$ ,  $B(E1)$ , and  $B(M1)$  values. ]

### I. INTRODUCTION

In recent years the level structure of  $^{77}\text{Se}$  has been the subject of numerous spectroscopic investigations employing the  $(d, p)$  and  $(d, t)$  reactions,<sup>1,2</sup> Coulomb excitation,<sup>3</sup> and  $(n, \gamma)$  spectroscopy.<sup>4,5</sup> The decay of 56-h  $^{77}\text{Br}$  to levels in  $^{77}\text{Se}$  has been studied by Monaro,<sup>6</sup> and Ardisson and Ythier.<sup>7</sup> More recently Sarantites and Erdal<sup>8</sup> studied the decay of  $^{77}\text{Br}$  by means of  $\gamma\gamma$ -coincidence measurements with two Ge(Li) detectors and by conversion-electron measurements with Si(Li) electron detectors. Although 44  $\gamma$  rays were assigned<sup>8</sup> to deexcite 14 levels in  $^{77}\text{Se}$ , the placement of some of the weaker transitions in the decay scheme remained tentative.

Attempts to interpret the level structure of  $^{77}\text{Se}$  have invoked a considerable variety of theoretical descriptions. For example, the 239.98 ( $\frac{3}{2}^-$ ) and 439.42 ( $\frac{3}{2}^-$ ) negative-parity states in  $^{77}\text{Se}$  have been interpreted<sup>6,3</sup> in terms of the core-particle model<sup>9</sup> and the pairing-plus-quadrupole model of Kisslinger and Sorensen<sup>10</sup> by Lin.<sup>2</sup> The negative- and positive-parity states in  $^{77}\text{Se}$  have

been interpreted in terms of the Nilsson model<sup>11</sup> for deformed nuclei by Engels.<sup>12</sup> Furthermore, the positive-parity states in  $^{77}\text{Se}$  have been also described by a variety of model calculations. Thus Ikegami and Sano<sup>13</sup> have used an extended pairing-plus-quadrupole model which includes admixtures from orbit in the next major shell. A different approach has been taken by Goswami, McDaniels, and Nalcioglu<sup>14</sup> who have used a different extended quasiparticle-phonon coupling theory in which they introduce a dipole-dipole interaction term of the form  $-\lambda J_c \cdot j_{qp}$  to supplement the static interaction terms of the form  $-\chi Q_c \cdot Q_{qp}$  where the subscripts  $c$  and  $qp$  refer to core phonon and quasiparticle, respectively. The large variety of models used in the interpretation of the levels in  $^{77}\text{Se}$  clearly indicates the difficulty that these theories face, particularly in explaining the low-lying positive-parity  $\frac{5}{2}^+$  and  $\frac{7}{2}^+$  states that occur in the nuclides where the protons or neutrons are filling the  $g_{9/2}$  shell. The purpose of the present work was to place the decay scheme on a more firm basis and to obtain values for the multipole mixing ratios in  $^{77}\text{Se}$  so that  $B(E2)$ ,

$B(M1)$ , and  $B(E1)$  values could be extracted for as many transitions as possible, with the hope of facilitating the choice between the various theoretical models proposed for the description of this nucleus. Employing two large Ge(Li) detectors, we were able to determine 14  $\delta(E2/M1)$  mixing ratios from  $\gamma\gamma$  directional correlations from 16 different cascades which involved common transitions in several cases. From these results in conjunction with previous lifetime measurements and  $B(E2)$  values obtained from Coulomb excitation<sup>3</sup> for certain transitions, we were able to establish the collective or single-particle character of several of the lower-lying levels in <sup>77</sup>Se.

## II. EXPERIMENTAL PROCEDURES

### A. Apparatus

For  $\gamma$ -ray singles measurements, a Ge(Li)-NaI(Tl) anti-Compton spectrometer was employed. This system consisted of a 42-cm<sup>3</sup> true coaxial Ge(Li) detector which was used in an anti-Compton arrangement with a 19.9-cm-diam by 12.7-cm-long annular NaI(Tl) detector. The Ge(Li) detector of this spectrometer had resolution (full width at half maximum) of 1.50 keV at 662 keV and 1.90 keV at 1332 keV. A detailed description of a similar arrangement and method of calibration has been given elsewhere.<sup>15</sup>

For the directional-correlation measurements, two closed-end coaxial Ge(Li) detectors with active volumes of 41 and 27 cm<sup>3</sup> with respective resolutions of 3.7 and 2.4 keV at 662 keV were employed. The 41-cm<sup>3</sup> Ge(Li) detector consisted of a crystal with dimensions 3.2-cm diam, 5.3-cm length, and 13-mm depletion depth. The 27-cm<sup>3</sup> Ge(Li) detector had dimensions 3.2-cm diam, 3.6-cm length, and 12-mm depletion depth. These dimensions and the position of each crystal in its cryostat relative to the covering can were determined by scanning with a collimated beam of  $\gamma$  rays as described in Ref. 16 and were needed in the evaluation of the correlation-attenuation factors due to the solid angle subtended by the detectors. In all the measurements, the 41- and 27-cm<sup>3</sup> detectors were mounted on a precision angular-correlation table and were positioned at a distance of 4.7 and 4.4 cm from the source, respectively. In order to substantially reduce the crystal-to-crystal Compton scattering the detectors were shielded with cylindrical 5.0-mm-thick lead absorbers. In addition, two 5-mm-thick "shutters" were mounted adjacent to the faces of each detector so that the face-to-face scattering could also be reduced. All the lead

shielding was lined with 1-mm cadmium to reduce the production of x rays.

### B. Attenuation factors for finite solid angles

Directional-correlation attenuation factors  $Q_2$  and  $Q_4$  for Ge(Li) detectors have been determined experimentally<sup>16</sup> for some typical detectors and tables for these have been compiled by Camp and Van Lehn.<sup>17</sup> Values for  $Q_2$  and  $Q_4$  for each detector used under the geometry described earlier were obtained by interpolation from the tables of Ref. 17. These values were checked (i) using the method of Ref. 16 and (ii) by measuring the correlation for the 248-123-keV  $4^+ \xrightarrow{E2} 2^+ \xrightarrow{E2} 0^+$  cascade in <sup>154</sup>Gd following <sup>154</sup>Eu decay. The  $Q_{22}$  and  $Q_{44}$  values used in this work are believed to be accurate to  $\approx 3$  and  $\approx 7\%$ , respectively.

### C. Data-acquisition system and data reduction

For  $\gamma\gamma$ -coincidence counting, standard electronics were employed in an arrangement described in Ref. 16 with resolving times between 95–105 nsec. For data acquisition, however, a Nuclear Data 4096-channel model 50/50 pulse-height analyzer was employed. This analyzer was interfaced to a PDP-8/L computer with an IBM computer compatible magnetic tape drive. This system was operated in a two-parameter mode. Eight digital gates per experiment were placed on the 27-cm<sup>3</sup> Ge(Li) detector axis to include the 238.98-, 249.77-, 281.65-, 297.23-, 384.99-, 439.47-, 484.57-, 520.69-, and 755.35-keV  $\gamma$  rays and their corresponding Compton backgrounds consisting of equal-width gates located above and below each peak. The spectra of the 41-cm<sup>3</sup> Ge(Li) movable detector were recorded in a 512-channel resolution which covered the range 30–800 keV. The correlations were obtained by normalizing the coincidence counts by the singles events recorded in the movable detector. To minimize dead-time losses due to high singles rates, the system was programmed to store singles events in the first group of 512 channels for 50 msec every 2.0 sec of the true live time. This arrangement further eliminated the need of any corrections due to sample decay during measurement at each angle. The contribution of random coincidence events to each gate was determined quantitatively by introducing a 60-cycle pulser to the test input of the preamplifier of the movable detector and determining the pulser counts in each spectrum. The random events were found always lower than 5% of the true events and were quantitatively subtracted from each gate.

Measurements were taken for 10<sup>4</sup> sec of live time at each angle with 15° intervals between 90

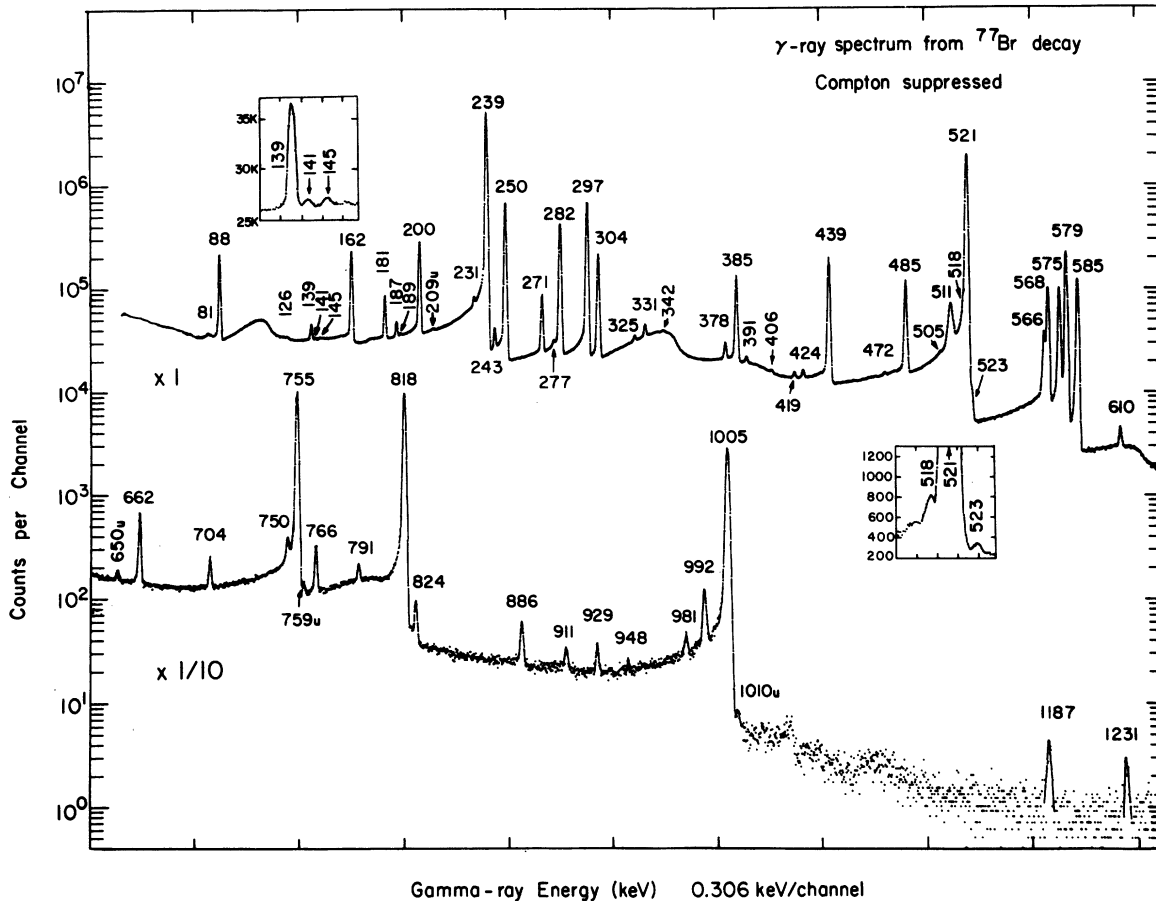


FIG. 1. Compton-suppressed singles  $\gamma$ -ray spectrum from 56-h  $^{77}\text{Br}$  decay obtained 24 h after bombardment. Peaks labeled u are unassigned.

and  $270^\circ$ . For each run, two or three complete sets of angles ( $90$ – $270^\circ$  every  $15^\circ$ ) were taken. Typical singles rates were between  $(0.5$ – $1.2) \times 10^4$  counts/sec and the total coincidence rates varied between  $100$ – $400$  counts/sec. During all measurements the liquid sources were sealed in Pyrex glass ampules (with a radius of  $2.0$  mm and  $7.0$  mm long), which were rotating with a period of  $12$  sec. In the present measurements no angular anisotropy of the apparatus could be detected.

The data were processed entirely with the aid of the PDP/8L on-line computer. From the spectrum in coincidence with each gated peak the random events were first subtracted and then the proper fraction of the Compton background was subtracted by using background spectra from one or both sides of the peak whenever possible. In the present experiments many correlations could be measured in two complementary ways, with the first  $\gamma$  ray recorded in the moving detector and the second in the stationary detector and vice versa. This permitted one to see whether the  $Q_{22}$  and  $Q_{44}$

factors were properly evaluated. By the choice of gates given above, it was possible to analyze only areas from nonoverlapping coincidence peaks.

#### D. Sources

The  $^{77}\text{Br}$  sources were prepared by the  $^{75}\text{As}(\alpha, 2n)^{77}\text{Br}$  reaction, using  $22$ -MeV  $\alpha$  particles from the Washington University cyclotron on  $\text{As}_2\text{O}_3$  targets. In all cases the sources were mounted in HBr solution and were purified radiochemically employing the procedure given in Ref. 8. Only the  $249.65$ -keV level has a relatively long lifetime<sup>6</sup> ( $9.3$  nsec) to be a possible candidate for attenuation of the correlations due to perturbations of the intermediate state from internal fields. Although the use of sources in the form of HBr solution minimizes such perturbations, some residual attenuation of the observed correlation involving the  $249.65$ -keV state is believed to have been observed and this will be discussed in conjunction with the presentation of the data.

TABLE I. Energy and relative intensity of the  $\gamma$  rays following  $^{77}\text{Br}$  decay from singles measurements under collimated anti-Compton arrangement and from high-resolution singles measurements with a Ge(Li) x-ray detector.

Transition	$\gamma$ -ray energy	Transition energy	$\gamma$ -ray energy	Relative $\gamma$ -ray intensity	
	in keV (this work)	from the scheme in keV (this work) <sup>a</sup>	in keV from Ref. 8	This work	Ref. 8
7 $\rightarrow$ 6	80.9 $\frac{1}{7}$ <sup>b</sup>	81.1 $\frac{1}{7}$ <sup>b</sup>		0.09 $\frac{3}{5}$ <sup>b</sup>	
4 $\rightarrow$ 1	87.59 $\frac{7}{8}$	87.82 $\frac{10}{10}$	87.8 $\frac{1}{1}$ <sup>b</sup>	6.06 $\frac{10}{5}$	5.36 $\frac{20}{5}$ <sup>b</sup>
5 $\rightarrow$ 2	125.57 $\frac{8}{8}$	125.78 $\frac{22}{22}$		0.040 $\frac{5}{5}$	
5 $\rightarrow$ 1	138.95 $\frac{9}{9}$	138.95 $\frac{13}{13}$	139.2 $\frac{1}{1}$	0.56 $\frac{2}{2}$	0.49 $\frac{5}{5}$
8 $\rightarrow$ 6	141.1 $\frac{3}{3}$	141.48 $\frac{13}{13}$		0.011 $\frac{3}{3}$	
11 $\rightarrow$ 9	144.5 $\frac{1}{1}$	144.65 $\frac{21}{21}$		0.025 $\frac{5}{5}$	
1 $\rightarrow$ 0	161.83 $\frac{8}{8}$	161.83 $\frac{8}{8}$	161.9 $\frac{1}{1}$	4.77 $\frac{8}{8}$	5.2 $\frac{2}{2}$
13 $\rightarrow$ 11	180.68 $\frac{7}{7}$	180.73 $\frac{6}{6}$	180.6 $\frac{1}{1}$	1.23 $\frac{3}{3}$	1.31 $\frac{8}{8}$
13 $\rightarrow$ 10	187.26 $\frac{8}{8}$	187.30 $\frac{6}{6}$	187.0 $\frac{1}{1}$	0.25 $\frac{1}{1}$	0.33 $\frac{4}{4}$
6 $\rightarrow$ 4	189.57 $\frac{21}{21}$	189.77 $\frac{8}{8}$		0.010 $\frac{5}{5}$	
6 $\rightarrow$ 3	200.40 $\frac{7}{7}$	200.44 $\frac{9}{9}$	200.4 $\frac{1}{1}$	5.25 $\frac{20}{20}$	5.3 $\frac{4}{4}$
12 $\rightarrow$ 9	231.49 $\frac{13}{13}$	231.70 $\frac{22}{22}$	231.5 $\frac{5}{5}$	0.27 $\frac{2}{2}$	0.43 $\frac{5}{5}$
3 $\rightarrow$ 0	238.98 $\frac{7}{7}$	238.98 $\frac{7}{7}$	238.9 $\frac{1}{1}$	100.00	100.00
11 $\rightarrow$ 8	243.35 $\frac{8}{8}$	243.45 $\frac{12}{12}$	243.8 $\frac{5}{5}$	0.16 $\frac{2}{2}$	0.19 $\frac{3}{3}$
4 $\rightarrow$ 0	249.77 $\frac{7}{7}$	249.65 $\frac{6}{6}$	249.7 $\frac{1}{1}$	12.9 $\frac{3}{3}$	12.4 $\frac{5}{5}$
7 $\rightarrow$ 4	270.83 $\frac{7}{7}$	270.98 $\frac{8}{8}$	270.6 $\frac{1}{1}$	1.39 $\frac{5}{5}$	1.30 $\frac{4}{4}$
6 $\rightarrow$ 1	277.47 $\frac{15}{15}$	277.59 $\frac{9}{9}$	277.4 $\frac{6}{6}$	0.14 $\frac{1}{1}$	0.16 $\frac{6}{6}$
7 $\rightarrow$ 3	281.65 $\frac{7}{7}$	281.65 $\frac{9}{9}$	281.6 $\frac{1}{1}$	9.9 $\frac{2}{2}$	9.3 $\frac{4}{4}$
10 $\rightarrow$ 7	297.23 $\frac{8}{8}$	297.15 $\frac{6}{6}$	297.2 $\frac{1}{1}$	18.0 $\frac{8}{8}$	16.0 $\frac{3}{3}$
11 $\rightarrow$ 7	303.76 $\frac{9}{9}$	303.72 $\frac{6}{6}$	303.8 $\frac{1}{1}$	5.1 $\frac{1}{1}$	4.76 $\frac{9}{9}$
13 $\rightarrow$ 9	325.08 $\frac{11}{11}$	325.38 $\frac{21}{21}$		0.10 $\frac{2}{2}$	
8 $\rightarrow$ 4	331.23 $\frac{9}{9}$	331.25 $\frac{13}{13}$	331.4 $\frac{1}{1}$	0.29 $\frac{3}{3}$	0.31 $\frac{6}{6}$
8 $\rightarrow$ 3	342.08 $\frac{24}{24}$	341.92 $\frac{13}{13}$		0.027 $\frac{5}{5}$	
10 $\rightarrow$ 6	378.45 $\frac{9}{9}$	378.36 $\frac{7}{7}$	378.5 $\frac{1}{1}$	0.26 $\frac{2}{2}$ <sup>c</sup>	0.23 $\frac{7}{7}$
9 $\rightarrow$ 5	378.45 $\frac{9}{9}$	378.92 $\frac{23}{23}$		0.04 $\frac{3}{3}$ <sup>c</sup>	
11 $\rightarrow$ 6	384.99 $\frac{8}{8}$	384.93 $\frac{7}{7}$	385.1 $\frac{1}{1}$	3.62 $\frac{10}{10}$	3.04 $\frac{9}{9}$
12 $\rightarrow$ 7	390.97 $\frac{11}{11}$	390.77 $\frac{9}{9}$		0.097 $\frac{11}{11}$	
8 $\rightarrow$ 2	405.87 $\frac{22}{22}$	405.90 $\frac{23}{23}$		0.032 $\frac{6}{6}$	
8 $\rightarrow$ 1	419.15 $\frac{19}{19}$	419.07 $\frac{13}{13}$	419.4 $\frac{2}{2}$	0.071 $\frac{9}{9}$	0.069 $\frac{10}{10}$
13 $\rightarrow$ 8	424.22 $\frac{15}{15}$	424.18 $\frac{12}{12}$		0.095 $\frac{10}{10}$	
6 $\rightarrow$ 0	439.47 $\frac{6}{6}$	439.42 $\frac{6}{6}$	439.7 $\frac{1}{1}$	6.77 $\frac{15}{15}$	6.2 $\frac{2}{2}$
12 $\rightarrow$ 6	472.03 $\frac{23}{23}$	471.98 $\frac{10}{10}$	472.5 $\frac{11}{11}$	0.034 $\frac{9}{9}$	0.073 $\frac{18}{18}$
13 $\rightarrow$ 7	484.57 $\frac{7}{7}$	484.45 $\frac{6}{6}$	484.8 $\frac{1}{1}$	4.33 $\frac{10}{10}$	3.65 $\frac{7}{7}$
9 $\rightarrow$ 2	504.53 $\frac{23}{23}$	504.70 $\frac{28}{28}$		0.039 $\frac{8}{8}$	
9 $\rightarrow$ 1	517.9 $\frac{4}{4}$	517.9 $\frac{2}{2}$		0.7 $\frac{2}{2}$	
7 $\rightarrow$ 0	520.69 $\frac{6}{6}$	520.63 $\frac{5}{5}$	521.0 $\frac{1}{1}$	97.0 $\frac{15}{15}$	90.6 $\frac{2}{2}$
11 $\rightarrow$ 5	523.4 $\frac{2}{2}$	523.57 $\frac{12}{12}$		0.17 $\frac{3}{3}$	
13 $\rightarrow$ 6	565.91 $\frac{19}{19}$	565.66 $\frac{7}{7}$	566.5 $\frac{4}{4}$	1.85 $\frac{6}{6}$	1.65 $\frac{10}{10}$
10 $\rightarrow$ 4	567.90 $\frac{8}{8}$	568.13 $\frac{7}{7}$	568.6 $\frac{3}{3}$	3.71 $\frac{8}{8}$	3.23 $\frac{16}{16}$
11 $\rightarrow$ 4	574.64 $\frac{8}{8}$	574.70 $\frac{7}{7}$	575.1 $\frac{2}{2}$	5.14 $\frac{10}{10}$	4.25 $\frac{9}{9}$
10 $\rightarrow$ 3	578.91 $\frac{7}{7}$	578.80 $\frac{8}{8}$	579.4 $\frac{1}{1}$	12.8 $\frac{3}{3}$	10.8 $\frac{2}{2}$
11 $\rightarrow$ 3	585.48 $\frac{7}{7}$	585.37 $\frac{8}{8}$	585.9 $\frac{1}{1}$	6.79 $\frac{14}{14}$	4.87 $\frac{10}{10}$
12 $\rightarrow$ 5	610.39 $\frac{8}{8}$	610.62 $\frac{14}{14}$	610.7 $\frac{7}{7}$	0.093 $\frac{9}{9}$	0.10 $\frac{1}{1}$
11 $\rightarrow$ 1	662.43 $\frac{9}{9}$	662.52 $\frac{7}{7}$	663.0 $\frac{1}{1}$	0.35 $\frac{1}{1}$	0.44 $\frac{3}{3}$
13 $\rightarrow$ 5	704.09 $\frac{12}{12}$	704.30 $\frac{12}{12}$	704.6 $\frac{2}{2}$	0.069 $\frac{8}{8}$	0.10 $\frac{1}{1}$
12 $\rightarrow$ 1	749.55 $\frac{10}{10}$	749.57 $\frac{11}{11}$	750.6 $\frac{6}{6}$	0.128 $\frac{14}{14}$	0.19 $\frac{3}{3}$
13 $\rightarrow$ 4	755.35 $\frac{7}{7}$	755.43 $\frac{7}{7}$	756.0 $\frac{1}{1}$	7.22 $\frac{14}{14}$	5.5 $\frac{1}{1}$
13 $\rightarrow$ 3	766.11 $\frac{8}{8}$	766.10 $\frac{8}{8}$	767.0 $\frac{1}{1}$	0.18 $\frac{1}{1}$	0.18 $\frac{1}{1}$
15 $\rightarrow$ 6	791.26 $\frac{11}{11}$	791.20 $\frac{15}{15}$	791.9 $\frac{3}{3}$	0.040 $\frac{9}{9}$	0.049 $\frac{7}{7}$
10 $\rightarrow$ 0	817.79 $\frac{6}{6}$	817.78 $\frac{4}{4}$	817.5 $\frac{1}{1}$	9.0 $\frac{2}{2}$	7.8 $\frac{2}{2}$
11 $\rightarrow$ 0	824.28 $\frac{12}{12}$	824.35 $\frac{4}{4}$	825.1 $\frac{1}{1}$	0.057 $\frac{6}{6}$	0.055 $\frac{8}{8}$

TABLE I (Continued)

Transition	$\gamma$ -ray energy	Transition energy	$\gamma$ -ray energy	Relative $\gamma$ -ray intensity	
	in keV (this work)	from the scheme in keV (this work) <sup>a</sup>	in keV from Ref. 8	This work	Ref. 8
14 $\rightarrow$ 5	885.71 <u>10</u>	885.71 <u>19</u>	886.4 <u>2</u>	0.036 <u>4</u>	0.034 <u>5</u>
12 $\rightarrow$ 0	911.36 <u>26</u>	911.40 <u>8</u>	911.8 <u>2</u>	0.011 <u>2</u>	0.023 <u>3</u>
15 $\rightarrow$ 5	929.38 <u>32</u>	929.84 <u>19</u>		0.012 <u>4</u>	
14 $\rightarrow$ 3	947.5 <u>4</u>	947.51 <u>17</u>		0.003 <u>1</u>	
15 $\rightarrow$ 4	980.81 <u>37</u>	980.97 <u>15</u>		0.016 <u>3</u>	
15 $\rightarrow$ 3	991.72 <u>20</u>	991.64 <u>16</u>	992.3 <u>2</u>	0.096 <u>5</u>	0.077 <u>5</u>
13 $\rightarrow$ 0	1005.05 <u>6</u>	1005.08 <u>4</u>	1005.7 <u>2</u>	4.00 <u>8</u>	3.15 <u>6</u>
14 $\rightarrow$ 0	1186.8 <u>3</u>	1186.55 <u>13</u>		0.007 <u>2</u>	
15 $\rightarrow$ 0	1230.5 <u>2</u>	1230.62 <u>14</u>		0.004 <u>1</u>	

<sup>a</sup> Values obtained as difference between the level energies, which in turn were obtained as weighted averages of the sums of the  $\gamma$  rays that lead to each level.

<sup>b</sup> Uncertainties (underlined) refer to the last given significant figures.

<sup>c</sup> Intensity estimated from the coincidence spectrum.

### III. RESULTS

#### A. Construction of the $^{77}\text{Br}$ decay scheme

A Compton-suppressed  $\gamma$ -ray spectrum of good statistical quality taken for a period of 20 h from a  $^{77}\text{Br}$  source 24 h after bombardment is shown in Fig. 1. The  $\gamma$  peaks were identified with the decay of  $^{77}\text{Br}$  by taking 20-h spectra consecutively for about 120 h and comparing the peak intensities relative to the 238.98-keV  $\gamma$  ray. The energy of the most intense  $\gamma$  rays was determined from five spectra which were taken by counting standard sources of  $^{57}\text{Co}$ ,  $^{133}\text{Ba}$ ,  $^{125}\text{Sb}$ ,  $^{137}\text{Cs}$ ,  $^{54}\text{Mn}$ , and  $^{60}\text{Co}$  together with  $^{77}\text{Br}$  samples. A set of five separate spectra from pure  $^{77}\text{Br}$  samples was used to determine the energy of the weak peaks and the relative intensity of all the peaks. The energies were determined from calibration functions obtained by fitting a cubic equation by the least-squares technique to the standards. The relative intensities of the  $\gamma$  rays were determined from full-energy peak areas using a detector efficiency curve obtained by means of calibrated sources<sup>18</sup> of  $^{241}\text{Am}$ ,  $^{57}\text{Co}$ ,  $^{203}\text{Hg}$ ,  $^{22}\text{Na}$ ,  $^{137}\text{Cs}$ ,  $^{54}\text{Mn}$ ,  $^{60}\text{Co}$ , and sources with well-known relative intensities of  $^{133}\text{Ba}$ ,  $^{125}\text{Sb}$ , and  $^{56}\text{Co}$ . The energy and intensity of the  $\gamma$  rays that have been included in the decay scheme proposed for  $^{77}\text{Br}$  are summarized in columns 2 and 5 of Table I. The third column gives the  $\gamma$ -ray energies determined from the proposed decay scheme as differences between established levels, the energy of which was obtained as a weighted average of the  $\gamma$ -ray energy sums leading to each level. The fourth and sixth columns of Table I give the energies and intensities from Ref. 8. A progressively increasing difference not exceeding  $\approx 0.6$  keV is observed for

$\gamma$  rays above  $\approx 400$  keV. Furthermore, there is a systematic difference in the measured  $\gamma$ -ray intensities between the present measurements and those of Ref. 8 with the latter being lower by 10–15% for  $\gamma$  rays above  $\approx 300$  keV. We believe that the present values are more accurate due to the large number of standard sources employed. The  $\gamma$  rays at 20.6, 77, 682.3, and 843.8 keV reported in Ref. 8 were not seen in the present experiments, while new  $\gamma$  rays at 80.9, 125.57, 141.1, 144.5, 189.57, 325.08, 342.08, 390.97, 405.87, 424.22, 504.53, 517.9, 523.4, 929.38, 947.5, 980.81, 1186.8, and 1230.5 keV were observed and were incorporated in the proposed decay scheme.

The scheme proposed for the decay of  $^{77}\text{Br}$  is shown in Fig. 2 and in general is in agreement with the results of Refs. 4 and 8. Here only the differences and the additions will be discussed.

The isomeric  $\frac{7}{2}^+$  level at 161.83 keV is well established (see discussion in Ref. 8), while a ( $\frac{9}{2}^+$ ) level at 175.0 keV proposed by Rabenstein and Vonach<sup>4</sup> appears to be populated also in the decay of  $^{77}\text{Br}$  via  $\gamma$  transitions at 125.57, 405.87, and 504.53 keV from well-established levels<sup>4, 8</sup> at 300.78, 580.90, and 679.7 keV, respectively.

A weak  $\gamma$  ray at 77 keV reported<sup>8</sup> to deexcite the 238.98-keV level was not observed in this work, while a weak  $\gamma$  ray at 189.57 keV was placed between the 439.42- and 249.65-keV levels on grounds of good energy agreement.

Weak  $\gamma$  rays at 80.9, 342.08, and 405.87 keV were observed and were assigned as in Ref. 4 to deexcite the 520.59- and 580.90-keV levels, respectively. An additional weak  $\gamma$  ray at 141.1 keV was assigned on energy grounds to deexcite the 580.90-keV level.

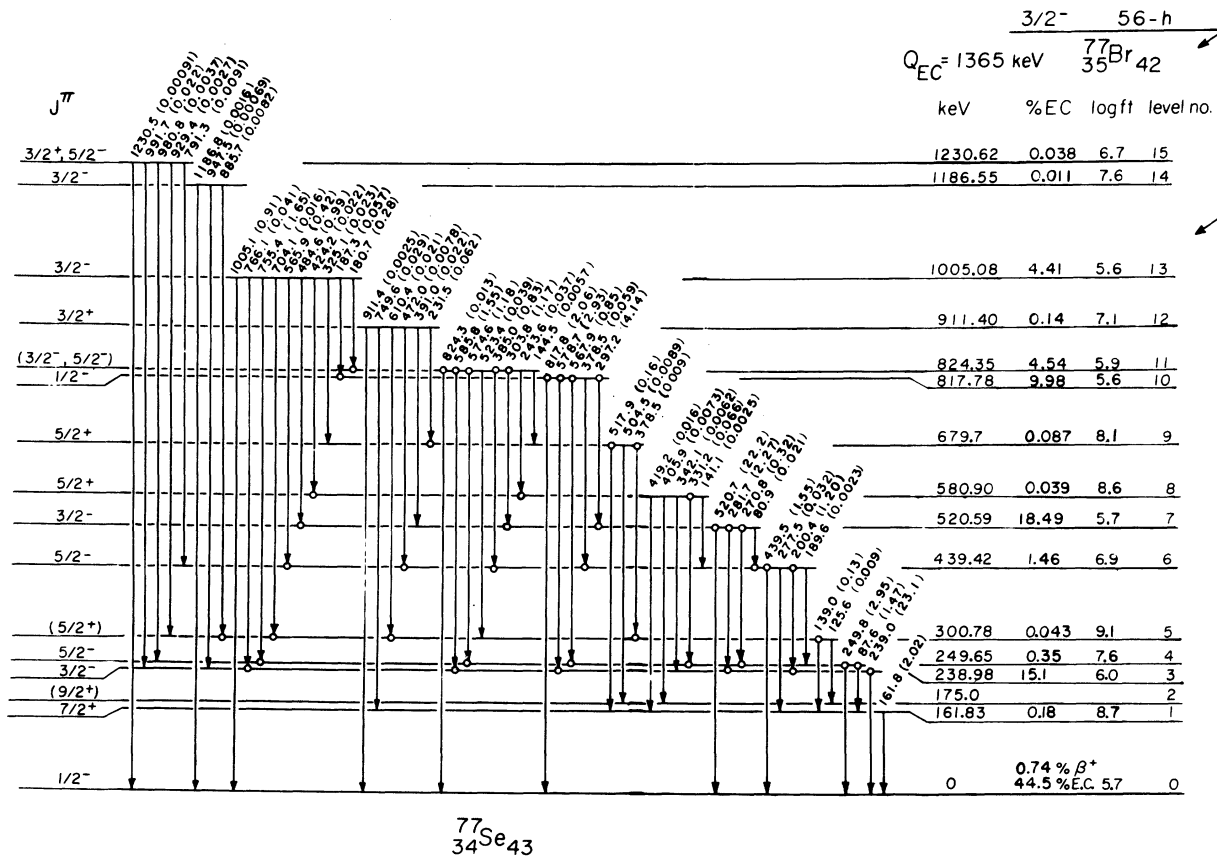


FIG. 2. Proposed decay scheme for 56-h  $^{77}\text{Br}$ . The energies are given in keV and the intensities are given in parentheses expressed per 100 decays.

A  $\gamma$  ray at 231.5 keV previously reported<sup>8</sup> to depopulate a 752.2-keV level, is now placed<sup>4</sup> to deexcite the 911.40-keV level, thus explaining the coincidences observed with the 518-527-keV gate<sup>8</sup> as due to the 231.49-517.9-keV  $\gamma\gamma$  cascade. The 517.9-keV  $\gamma$  ray was resolved in this work from the very intense 520.69-keV  $\gamma$  ray (insert in Fig. 1). A weak 504.53-keV  $\gamma$  ray was also seen in this work and in agreement with Ref. 4 was assigned to deexcite the 679.7-keV level.

A 682.3-keV  $\gamma$  ray previously assigned<sup>8</sup> to depopulate a 682.3-keV level was not observed in this work, although that level should be identified with the 679.7-keV level.<sup>1,2</sup> Three  $\gamma$  rays at 378.45, 504.53, and 517.9 keV were assigned to deexcite the 679.7-keV level. Of these, the 378.45-keV  $\gamma$  ray was observed in weak coincidence with the 231.49- and 138.95-keV  $\gamma$  rays, and its intensity was estimated from the coincidence spectra.

A  $\gamma$  ray at 656.3 keV was assigned earlier<sup>8</sup> to deexcite the 817.78-keV level. This  $\gamma$  ray was also observed in some of the present spectra but it is not believed to be associated with the  $^{77}\text{Br}$

decay.

The well-established 824.35-keV level was assigned<sup>8</sup> to deexcite via a 663.0-keV transition. This transition which, in the present work, is found at 662.43 keV was not observed in coincidence with the 180.68-keV  $\gamma$  ray that is known<sup>8</sup> to populate the 824.35-keV level (Fig. 4 in Ref. 8). We must therefore conclude that this 662.43-keV  $\gamma$  ray deexcites some other level in  $^{77}\text{Se}$ . The weak 144.5- and 523.4-keV  $\gamma$  rays were tentatively assigned to deexcite the 824.35-keV level on grounds of good energy agreement.

In addition to the 231.49-keV  $\gamma$  ray, another weak 390.97-keV  $\gamma$  ray was assigned on energy grounds to deexcite the well-established level<sup>8,4</sup> at 911.40 keV.

The level<sup>3,4</sup> at 1186.55 keV was observed to decay by the 885.71-, 947.5-, and 1186.8-keV  $\gamma$  rays.

Finally, a level at 1230.62 keV in  $^{77}\text{Se}$  was observed to deexcite by five weak  $\gamma$  rays at 791.26, 929.38, 980.81, 991.72, and 1230.5 keV. This level was also observed in the  $(n, \gamma)$  work of Rabenstein and Vonach.<sup>4</sup>

In the proposed scheme, the ratio  $I(\gamma^+)/I(239.0\gamma)$  of 0.0635 20 of Ref. 8 was adopted in order to calculate the direct population of the  $^{77}\text{Se}$  ground state. The intensities given in parentheses in Fig. 2 are transition intensities given per 100 decays and were obtained from  $\gamma$ -ray intensities by correcting all transitions below 521 keV for internal conversion by using the  $K$  conversion coefficients of Ref. 8 and the  $K$ -shell and  $L$ -shell conversion coefficients of Hager and Seltzer<sup>19</sup> assuming an  $M1$  character for the transitions of unknown multipolarity. For most of such cases the corrections were  $\leq 1.0\%$ .

Table II summarizes the proposed level energies, the percent electron capture (EC) and  $\beta^+$  populations, the deduced  $\log ft$  values<sup>20</sup> using<sup>21</sup>  $Q_{\text{EC}} = 1365$  keV and the assigned  $J^\pi$  values to each proposed level.

#### B. Angular-correlation measurements

The directional correlations for 16 individual  $\gamma\gamma$  cascades involving 14  $\gamma$  rays were measured. The obtained correlations were analyzed by fitting of the data by least-squares techniques to the function

$$W(\theta_d) = A_{00}[1 + A_{22}Q_{22}P_2(\cos\theta_d) + A_{44}Q_{44}P_4(\cos\theta_d)], \quad (1)$$

where the attenuation factors  $Q_{hh}$  have been discussed in Refs. 16 and 17, and the  $A_{hh}$  coefficients are related to the  $J^\pi$  and multipole-mixing-ratio values involved as described by Rose and Brink.<sup>22</sup> In some cases correlations involving one intermediate unobserved transition were measured. In such cases the theoretical  $A_{hh}$  coefficients were obtained as  $A_h(J_2J_1\delta_1) U_h(J_2J_3\delta_2) A_h(J_3J_4\delta_3)$  with the linking parameters  $U_h$  as tabulated by Rose and Brink.<sup>22</sup>

In Figs. 3 and 4 we show the correlations that were measured, plotted as a function of  $\cos^2\theta_d$ . The solid curves in Figs. 3 and 4 are the theoretical correlations for the adopted spin sequences which gave the  $J^\pi$  and  $\delta$  values shown in Table III and correspond to the minimum values of  $\chi^2$  shown in parentheses after each spin sequence in the figures. In Figs. 3 and 4 after the transition energies in keV, are given in parentheses the level numbers that help identify the cascades. The dashed or dotted curves show the theoretical correlations that give the best fit for alternate spin sequences, which were rejected as improbable (see Sec. C. below).

In Table III the first column gives the  $\gamma\gamma$  cascade in keV with the spin sequence denoted in parentheses. In columns 2 and 3 of Table III are given the experimental values of the  $A_{22}$  and

TABLE II. Assignment of  $\log ft$  and  $J^\pi$  values to levels in  $^{77}\text{Se}$ .

Level no.	Level energy (keV)	% electron capture	$\log ft^a$	$J^\pi$
0	0	44.5 <u>22</u>	5.7	$\frac{1}{2}^-$
1	161.83 <u>7</u>	0.18 <u>12</u>	$8.7^{+5}_{-2}$	$\frac{7}{2}^+$
2	175.0 <u>2</u>	...	...	$(\frac{9}{2}^+)$
3	238.98 <u>7</u>	15.1 <u>4</u>	6.0	$\frac{3}{2}^-$
4	249.65 <u>6</u>	0.35 <u>9</u>	7.6	$\frac{5}{2}^-$
5	300.78 <u>11</u>	0.043 <u>11</u>	9.1	$(\frac{5}{2}^+)$
6	439.42 <u>6</u>	1.46 <u>6</u>	6.9	$\frac{3}{2}^-$
7	520.59 <u>5</u>	18.5 <u>4</u>	5.7	$\frac{3}{2}^-$
8	580.90 <u>11</u>	0.039 <u>9</u>	8.6	$\frac{5}{2}^+$
9	679.7 <u>2</u>	0.087 <u>47</u>	$8.1^{+3}_{-2}$	$\frac{3}{2}^+$
10	817.78 <u>5</u>	10.0 <u>2</u>	5.6	$\frac{3}{2}^-$
11	824.35 <u>5</u>	4.54 <u>5</u>	5.9	$(\frac{3}{2}^-, \frac{5}{2}^-)$
12	911.40 <u>8</u>	0.14 <u>1</u>	7.1	$\frac{3}{2}^+$
13	1005.08 <u>5</u>	4.41 <u>5</u>	5.6	$\frac{3}{2}^-$
14	1186.55 <u>13</u>	0.011 <u>1</u>	7.6	$\frac{3}{2}^-$
15	1230.62 <u>14</u>	0.038 <u>3</u>	6.7	$\frac{3}{2}^+, \frac{5}{2}^-$

<sup>a</sup> Uncertainties are smaller than 0.1 unit unless otherwise indicated.

$A_{44}$  coefficients as obtained from Eq. (1) by least-squares techniques, and in parentheses are given the  $Q_{22}$  and  $Q_{44}$  values used. Columns 4 and 5 give the values of  $A_{hh}$  obtained at minimum  $\chi^2$  when the  $\delta$  values in the theoretical coefficients  $A_{hh}$  of Eq. (1) are varied and the  $\chi^2$  for the fit to the data is evaluated. Column 6 gives the minimum value of  $\chi^2$  obtained for the  $\delta$  values for the upper and lower transitions as given in columns 7 and 8, respectively.

For 5 of the 16 correlations listed in Table III, the 9.3-nsec 249.65-keV state is involved as the intermediate state. Such a lifetime is sufficiently long to permit spin reorientation due to internal fields. This would reduce the correlations from their unperturbed values and would become most apparent in the strongly correlated cascades 755.35–249.77-keV and 567.90–249.77-keV cascades. No evidence for such an effect was found by Monaro<sup>6</sup> for the 755.35–249.77-keV correlation, but Engels *et al.*<sup>23</sup> reported evidence for attenuation of this correlation by internal fields. Furthermore, the 817.78-keV level has been shown independently<sup>5</sup> from circular-polarization measurements to be  $\frac{1}{2}^-$ . Since the 249.65-keV level undoubtedly<sup>4,8</sup> is  $\frac{5}{2}^-$ , the 567.90–249.77-keV cascade is established as  $\frac{1}{2}^- - \frac{5}{2}^- \rightarrow \frac{1}{2}^-$ . The present mea-

surement of this correlation [Fig. 4(a)] would not be consistent with this spin sequence if the correlation were assumed unperturbed ( $\chi^2_{\min} = 8.6$ ). If however, attenuation coefficients  $G_R$  of 0.75 are assumed, the present results become consistent with the  $\frac{1}{2}^- \rightarrow \frac{3}{2}^- \rightarrow \frac{1}{2}^-$  sequence with  $\chi^2_{\min} = 1.4$ . Such a value for the perturbation coefficients for lifetimes of  $\sim 10$  nsec are not uncommon. Although the assumption of such a perturbation does not alter the possible spin assignments, it does affect the values deduced for the multipole mixing ratios for the 270.83-, 574.64-, and 755.35-keV transitions. These values for  $\delta(E2/M1)$  based on attenuation coefficients of 0.75 are given in parentheses in the last two columns of Table III.

### C. Assignment of $J^\pi$ values

The  $J^\pi$  values for the ground state, 161.83-, 239.98-, 249.65-, and 439.42-keV states are well

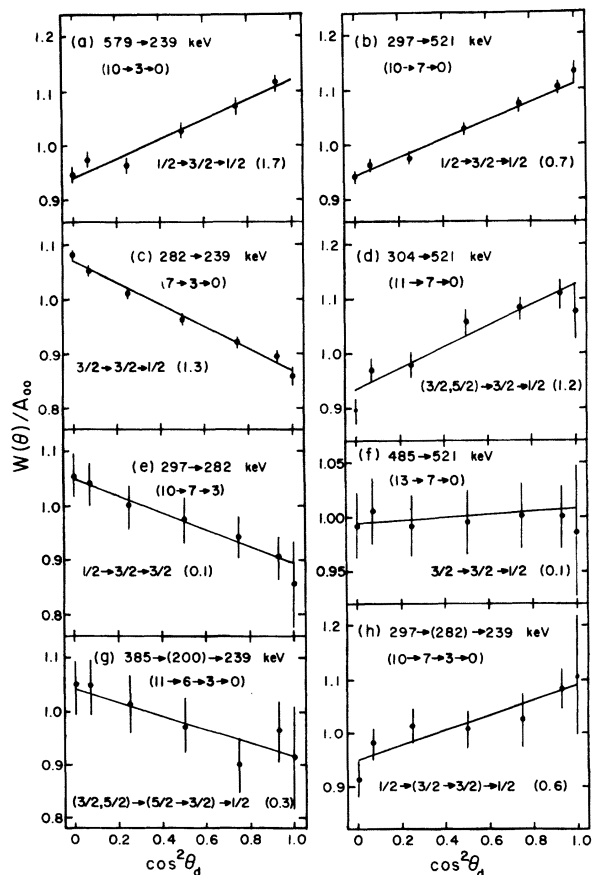


FIG. 3. Angular correlations of the  $\gamma$  cascades indicated in keV for the transitions identified by the integers in parentheses. The quantity  $W(\theta)/A_{00}$  is plotted vs  $\cos^2\theta_d$ . The solid curves are the theoretical correlations for the  $\delta$  values that gave the minimum  $\chi^2$  value shown in parentheses after the spin sequence.

established<sup>8,4,24</sup> as  $\frac{1}{2}^-$ ,  $\frac{7}{2}^+$ ,  $\frac{3}{2}^-$ ,  $\frac{5}{2}^-$ , and  $\frac{5}{2}^-$ , respectively. The  $\frac{3}{2}^- \rightarrow \frac{1}{2}^-$  assignment for the 238.98-keV transition is further supported by the correlations from five cascades involving this transition, which yield internally consistent  $\delta(E2/M1)$  values (Table III). The  $\frac{5}{2}^- \rightarrow \frac{1}{2}^-$  character of the 249.77-keV transition is further supported from this work by the correlations from four cascades involving this transition. The  $\frac{3}{2}^-$  assignment for the 439.42-keV level is further supported by the results of at least three correlations involving the 200.40- and 439.47-keV  $\gamma$  rays. The  $\frac{9}{2}^+$  level at 175.0 keV proposed by Rabenstein and Vonach<sup>4</sup> was also seen to be populated by  $\gamma$  decay from the 300.78-, 580.90-, and 679.7-keV levels, which are shown below to be  $\frac{5}{2}^+$ .

The 300.78-keV level is most likely  $\frac{5}{2}^+$  and arguments for this have been given in Refs. 8

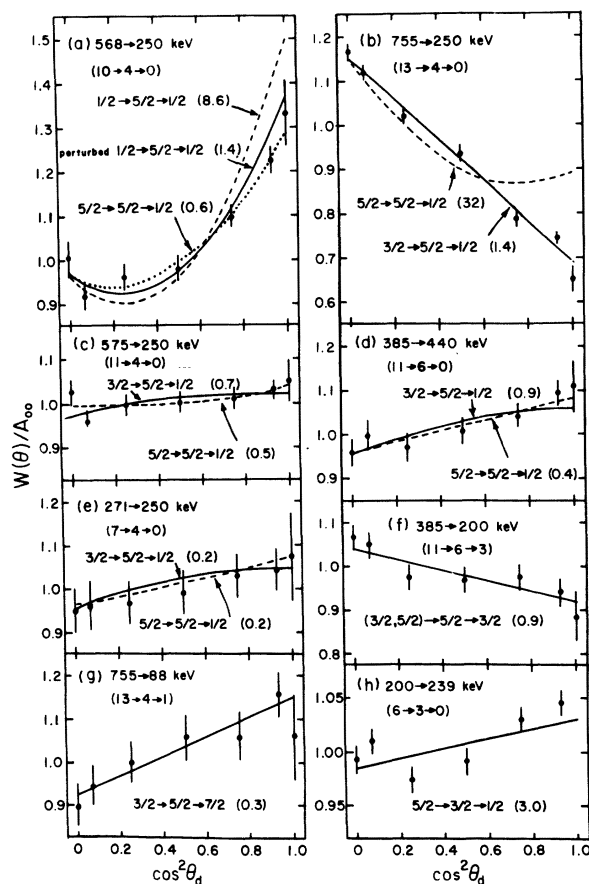


FIG. 4. Angular correlations of the  $\gamma$  cascades indicated in keV for the transitions identified by the integers in parentheses. The quantity  $W(\theta)/A_{00}$  is plotted vs  $\cos^2\theta_d$ . The solid curves are the theoretical correlations for the  $\delta$  values that gave the minimum  $\chi^2$  value shown in parentheses after the spin sequence. The dashed or dotted curves denote alternate spin sequences obtained also at minimum  $\chi^2$ .

TABLE III. Summary of the directional correlation results and of the deduced multipole mixing ratios for transitions in  $^{77}\text{Se}$ .

$\gamma$ - $\gamma$ cascade (keV) (Spin sequence) <sup>c</sup> Level sequence	Experimental values <sup>a</sup>		Theoretical values <sup>b</sup> at minimum $\chi^2$		Minimum $\chi^2$	Multipole mixing ratios $\delta(E2/M1)$	
	$A_{22}$ ( $Q_{22}$ )	$A_{44}$ ( $Q_{44}$ )	$A_{22}$	$A_{44}$		$\delta$ (upper)	$\delta$ (lower)
271-250 <sup>d</sup> ( $\frac{3}{2} \rightarrow \frac{5}{2} \rightarrow \frac{1}{2}$ )	0.080 <u>7</u>	0.016 <u>12</u>	0.076	-0.030	0.20	$0.27^{+4}_{-5}$	0.0 <sup>e</sup>
7 $\rightarrow$ 4 $\rightarrow$ 0	(0.875)	(0.638)	(0.104) <sup>f</sup>	(-0.036) <sup>f</sup>	(0.20)	$(0.30^{+5}_{-6})$	
568-250 <sup>d</sup> ( $\frac{1}{2} \rightarrow \frac{5}{2} \rightarrow \frac{1}{2}$ )	0.180 <u>27</u>	0.211 <u>47</u>	0.286	0.381	8.6	0.0 <sup>e</sup>	0.0 <sup>e</sup>
10 $\rightarrow$ 4 $\rightarrow$ 0	(0.877)	(0.642)	(0.284) <sup>f</sup>	(0.353) <sup>f</sup>	1.4	0.07 <sup>g</sup>	0.07 <sup>g</sup>
575-250 <sup>d</sup> ( $\frac{3}{2} \rightarrow \frac{5}{2} \rightarrow \frac{1}{2}$ )	0.024 <u>20</u>	0.029 <u>34</u>	0.027	-0.020	0.7	$0.22 \pm 6$	0.0 <sup>e</sup>
	(0.877)	(0.642)	(0.038) <sup>f</sup>	(-0.022) <sup>f</sup>	(0.7)	$(0.23 \pm 7)$	(0.0) <sup>e</sup>
or ( $\frac{5}{2} \rightarrow \frac{5}{2} \rightarrow \frac{1}{2}$ )			0.027	0.026	0.5	$-0.34^{+7}_{-8}$	0.0 <sup>e</sup>
11 $\rightarrow$ 4 $\rightarrow$ 0			(0.035) <sup>f</sup>	(0.024) <sup>f</sup>	(0.5)	$(-0.33^{+8}_{-9})$	(0.0) <sup>e</sup>
755-250 <sup>d</sup> ( $\frac{3}{2} \rightarrow \frac{5}{2} \rightarrow \frac{1}{2}$ )	-0.354 <u>21</u>	0.011 <u>37</u>	-0.349	-0.011	1.4	$-0.16^{+6}_{-5}$	0.0 <sup>e</sup>
13 $\rightarrow$ 4 $\rightarrow$ 0	(0.877)	(0.644)	(-0.466) <sup>f</sup>	(-0.039) <sup>f</sup>	(1.4)	$(-0.31^{+7}_{-6})$	(0.0) <sup>e</sup>
385-440 ( $\frac{3}{2} \rightarrow \frac{5}{2} \rightarrow \frac{1}{2}$ )	0.086 <u>14</u>	0.053 <u>24</u>	0.091	-0.033	0.9	$0.29^{+7}_{-6}$	0.0 <sup>e</sup>
	(0.878)	(0.645)					
or ( $\frac{5}{2} \rightarrow \frac{5}{2} \rightarrow \frac{1}{2}$ )			0.087	0.013	0.41	$-0.24^{+8}_{-7}$	0.0 <sup>e</sup>
11 $\rightarrow$ 6 $\rightarrow$ 0							
755-88 <sup>d</sup> ( $\frac{3}{2} \rightarrow \frac{5}{2} \rightarrow \frac{7}{2}$ )	0.177 <u>29</u>	-0.053 <u>55</u>	0.178	0.00	0.4	$0.18^{+14}_{-15}$	-0.09 $\pm$ 5
13 $\rightarrow$ 4 $\rightarrow$ 1	(0.857)	(0.595)	(0.237) <sup>f</sup>	(0.00) <sup>f</sup>	(0.4)	$(-0.34^{+16}_{-15})$	(-0.09 $\pm$ 5) <sup>f</sup>
385-200 ( $\frac{3}{2} \rightarrow \frac{5}{2} \rightarrow \frac{3}{2}$ )	-0.100 <u>26</u>	0.044 <u>45</u>	-0.088	0 or 0.044	0.9	$+0.33^{+11}_{-10}$	0.00 $\pm$ 14
	(0.874)	(0.635)					or $3.3^{+13}_{-24}$
or ( $\frac{5}{2} \rightarrow \frac{5}{2} \rightarrow \frac{3}{2}$ )			-0.088	0.00 or -0.011	0.9	$-0.21^{+7}_{-13}$	$0.04^{+19}_{-15}$
11 $\rightarrow$ 6 $\rightarrow$ 3							or $2.9^{+18}_{-10}$
200-239 ( $\frac{5}{2} \rightarrow \frac{3}{2} \rightarrow \frac{1}{2}$ )	0.033 <u>13</u>	0.059 <u>25</u>	0.034	0	3.0	$-0.02^{+11}_{-10}$	$-0.04^{+40}_{-26}$
6 $\rightarrow$ 3 $\rightarrow$ 0	(0.871)	(0.630)				or $-4.3^{+14}_{-18}$	or $1.88^{+245}_{-104}$
579-239 ( $\frac{1}{2} \rightarrow \frac{3}{2} \rightarrow \frac{1}{2}$ )	0.129 <u>14</u>	0.038 <u>25</u>	0.134	0	1.7	$0.16^{+3}_{-4}$	$0.09^{+12}_{-9}$
10 $\rightarrow$ 3 $\rightarrow$ 0	(0.877)	(0.642)				or $-2.6^{+2}_{-3}$	or $1.4^{+3}_{-2}$
282-239 ( $\frac{3}{2} \rightarrow \frac{3}{2} \rightarrow \frac{1}{2}$ )	-0.153 <u>6</u>	0.022 <u>12</u>	-0.150	0	1.3	$-0.12^{+3}_{-4}$	$0.14 \pm 4$
7 $\rightarrow$ 3 $\rightarrow$ 0	(0.874)	(0.638)				or $7.4^{+12}_{-8}$	or $1.28^{+10}_{-2}$

TABLE III (Continued)

$\gamma$ - $\gamma$ cascade (keV) (Spin sequence) <sup>c</sup> Level sequence	Experimental values <sup>a</sup>		Theoretical values <sup>b</sup> at minimum $\chi^2$		Minimum $\chi^2$	Multipole mixing ratios $\delta(E2/M1)$	
	$A_{22}$ ( $Q_{22}$ )	$A_{44}$ ( $Q_{44}$ )	$A_{22}$	$A_{44}$		$\delta$ (upper)	$\delta$ (lower)
297-282 ( $\frac{1}{2} \rightarrow \frac{3}{2} \rightarrow \frac{3}{2}$ ) 10 $\rightarrow$ 7 $\rightarrow$ 3	-0.119 <u>11</u> (0.876)	-0.007 <u>20</u> (0.642)	-0.120	0	0.09	$0.16^{+4}_{-5}$ or $-2.6^{+3}_{-4}$	$-0.11^{+6}_{-11}$ or $-2.6^{+6}_{-3}$
297-521 ( $\frac{1}{2} \rightarrow \frac{3}{2} \rightarrow \frac{1}{2}$ ) 10 $\rightarrow$ 7 $\rightarrow$ 0	0.127 <u>6</u> (0.878)	0.015 <u>11</u> (0.645)	0.128	0	0.7	$0.18^{+3}_{-4}$ or $-2.8 \pm 3$	$0.18^{+7}_{-9}$ or $1.2 \pm 2$
304-521 ( $\frac{3}{2} \rightarrow \frac{3}{2} \rightarrow \frac{1}{2}$ ) or ( $\frac{5}{2} \rightarrow \frac{3}{2} \rightarrow \frac{1}{2}$ ) 11 $\rightarrow$ 7 $\rightarrow$ 0	0.162 <u>19</u> (0.878)	-0.064 <u>33</u> (0.645)	0.145	0	1.2	$-0.44^{+5}_{-16}$ or $-6.3^{+26}_{-51}$	$0.07^{+25}_{-16}$ or $1.5 \pm 6$
485-521 ( $\frac{3}{2} \rightarrow \frac{3}{2} \rightarrow \frac{1}{2}$ ) 13 $\rightarrow$ 7 $\rightarrow$ 0	0.011 <u>10</u> (0.879)	-0.002 <u>18</u> (0.648)	0.010	0	0.12	$-0.27^{+4}_{-3}$	$0.17^{+6}_{-7}$ <sup>h</sup>
385-(200)-239 ( $\frac{3}{2} \rightarrow \frac{3}{2} \rightarrow \frac{3}{2} \rightarrow \frac{1}{2}$ ) or ( $\frac{5}{2} \rightarrow \frac{5}{2} \rightarrow \frac{3}{2} \rightarrow \frac{1}{2}$ ) 11 $\rightarrow$ 6 $\rightarrow$ 3 $\rightarrow$ 0	-0.115 <u>25</u> (0.876)	0.053 <u>44</u> (0.640)	-0.099	0	0.28	$0.36 \pm 11$ <sup>i</sup> $-0.19^{+14}_{-11}$ <sup>i</sup>	$-0.04 \pm 15$ or $1.9 \pm 7$ $0.07^{+35}_{-13}$ or $1.5^{+3}_{-8}$
297-(282)-239 ( $\frac{1}{2} \rightarrow \frac{3}{2} \rightarrow \frac{3}{2} \rightarrow \frac{1}{2}$ ) 10 $\rightarrow$ 7 $\rightarrow$ 3 $\rightarrow$ 0	0.106 <u>28</u> (0.875)	-0.019 <u>28</u> (0.639)	0.105	0	0.6	$-2.4 \leq \delta \leq 0.12$ <sup>j</sup>	$0.09^{+31}_{-23}$ or $1.4^{+10}_{-8}$

<sup>a</sup> Values of  $A_{k,k}$  from least-squares analysis of the data. The numbers in parentheses give the  $Q_{k,k}$  attenuation coefficients employed. Uncertainties (underlined) refer to the last given significant figures.

<sup>b</sup> Theoretical  $A_{22}$  coefficients for the spin sequence indicated, obtained with the  $\delta$  values given in the last two columns. When these  $\delta$  values are used, a minimum  $\chi^2$  value for the fit of Eq. (1) to the data is obtained.

<sup>c</sup> Spin sequence indicated in parentheses. When a spin sequence is not unique the possible sequences consistent with the present results are also included.

<sup>d</sup> Cascades involving the 249.65-keV 9.3-nsec state which exhibit perturbation effects.

<sup>e</sup> Transitions assumed to be pure  $E2$ .

<sup>f</sup> Values obtained assuming  $G_2 = G_4 = 0.75$ .

<sup>g</sup> Transitions allowed a small  $\delta(M3/E2)$  admixture.

<sup>h</sup> Values adopted from average of  $\delta_{521}$  obtained from 297-521 and 304-521 cascades.

<sup>i</sup> Value obtained employing  $\delta_{200} = 0.0$ .

<sup>j</sup> Limits derived with  $\delta_{282} = -0.11$ .

and 4.

The 520.59-keV level is now definitely established as  $\frac{3}{2}^-$  on the basis of the correlations shown in Figs. 3(b), 3(d)-3(f).

The 580.90-keV level is very weakly populated by electron capture and its high (8.6)  $\log ft$  value is consistent with a first-forbidden transition. This level decays to  $\frac{3}{2}^-$ ,  $\frac{5}{2}^-$ ,  $\frac{7}{2}^+$ , and possibly  $\frac{9}{2}^+$

levels below.<sup>4</sup> This limits the  $J^\pi$  value for this level to  $\frac{5}{2}^+$  as the most likely one.

The 679.7-keV level is populated by the ( $d, p$ ) reaction<sup>1,2</sup> with a  $L_n$  value of 2. This level is weakly populated by electron capture and was observed to decay to  $\frac{7}{2}^+$  and  $\frac{9}{2}^+$  states below. This information limits the  $J^\pi$  value for this level to  $\frac{5}{2}^+$ .

For the 817.78-keV level all the measured correlations for the cascades originating from this level are consistent with  $J^\pi$  of  $\frac{1}{2}^-$  or  $\frac{3}{2}^-$ . The circular-polarization measurements of Knerr and Vonach<sup>5</sup> limit the  $J^\pi$  for this level to  $\frac{1}{2}^-$ .

The correlations of four cascades originating from the 824.35-keV level were measured (Table III) and were all found consistent with a  $\frac{3}{2}^-$  or  $\frac{5}{2}^-$  assignment for this level. The fact that this level is very weakly populated<sup>4</sup> in the  $(n, \gamma)$  reaction supports the  $\frac{3}{2}^-$  assignment, although the lack of decay to the  $(\frac{7}{2}^+)$  161.83-keV level somewhat favors the  $\frac{3}{2}^-$  assignment.

The 911.40-keV level is weakly populated by electron capture, while it decays to  $\frac{1}{2}^-$ ,  $\frac{3}{2}^-$ ,  $\frac{5}{2}^-$ ,  $\frac{5}{2}^+$ , and  $\frac{7}{2}^+$  levels below. This limits the  $J^\pi$  assignment for this level to  $\frac{3}{2}^+$ .

The 1005.08-keV level is definitely established as  $\frac{3}{2}^-$  from the correlation of the (755-250)-keV cascade which is only consistent with a  $\frac{3}{2}^- \rightarrow \frac{5}{2}^- \rightarrow \frac{1}{2}^-$  sequence.

The 1186.55-keV level was found to be weakly populated by electron capture and it was seen in this to decay to the  $\frac{1}{2}^-$  ground and the  $\frac{5}{2}^+$  300.78-keV states. Additional branches for the decay of this level were reported by Rabenstein and Vonach<sup>4</sup> following the  $(n, \gamma)$  reaction. These authors<sup>4,5</sup> assign the 1186.55-keV level as  $\frac{3}{2}^-$ .

Finally, the 1230.62-keV level receives rather weak population by electron capture and it was observed to decay to  $\frac{1}{2}^-$ ,  $\frac{3}{2}^-$ ,  $\frac{5}{2}^-$ , and  $\frac{5}{2}^+$  states below. This information is sufficient to limit the  $J^\pi$  value for this level to either  $\frac{3}{2}^+$  or  $\frac{5}{2}^-$ .

#### IV. DISCUSSION

The scheme proposed for the decay of  $^{77}\text{Br}$  is in agreement with that proposed by Sarantites and Erdal<sup>8</sup> with the exception of the assignment of some of the weaker transitions as discussed in Sec. IIIA.. The decay properties of the levels in  $^{77}\text{Se}$  as observed in this work are also in good agreement with the independent results of Rabenstein and Vonach<sup>4</sup> employing the  $(n, \gamma)$  reaction with a few minor exceptions. Thus, Rabenstein and Vonach<sup>4</sup> assigned a  $\gamma$  ray at 279.2 keV to deexcite the 580.90-keV level. We have observed a  $(277.47 \pm 0.15)$ -keV  $\gamma$  ray and can place an intensity upper limit of  $\pm 0.25$  per 100 decays for a 280.1-keV  $\gamma$  ray, that could deexcite the 580.90-keV level.

The 378.45-keV line was found to be an unresolved doublet with an energy difference of  $\leq 0.3$  keV and not 1.1 keV as reported earlier.<sup>4</sup>

Two  $\gamma$  rays with an energy of 331.2 keV were assigned<sup>4</sup> to deexcite the 911.4- and 580.9-keV levels [Fig. 13(a) in Ref 4]. We find no evidence

for such a doublet and found no coincidence of the 331.23-keV  $\gamma$  ray with another  $\gamma$  ray of the same energy. Since the 331.23-keV  $\gamma$  ray was observed in coincidence with the 243.35-, and 424.22-keV  $\gamma$  rays it must deexcite the 580.90-keV level (see Fig. 2).

The angular correlations measured in this work provided several independent values for most of the transitions involved in the correlations. In Table IV are summarized the values of the deduced multipole mixing ratios obtained as weighted averages of the values reported in Table III. The first column in Table IV gives the level energy; the second column gives the weighted average value of the level lifetimes as reported in Refs. 3, 6, and 23-27; the third column gives the transition number in parentheses and transition energy in keV; the fourth column gives the spin sequence and the fifth column gives the multipole mixing ratios  $\delta(E2/M1)$  or the multipole character for the pure transitions as indicated; the last two columns give the  $B(E2)$ ,  $B(M1)$ , or  $B(E1)$  values deduced for the transitions from the 238.98-, 249.65-, 439.42-, and 520.59-keV levels given in Weisskopf units (W.u.) evaluated using the expression given in the Appendix of Ref. 28.

The  $\delta(E2/M1)$  values of  $0.13 \pm 0.04$  for the 238.98-keV transition is somewhat lower than  $0.18 \pm 0.03$  reported by Robinson *et al.*<sup>3</sup> For the 200.40-keV transition we find  $\delta(E2/M1) = 0.0 \pm 0.1$  consistent with  $0.05 \pm 0.03$  of Robinson *et al.*<sup>3</sup>

From the somewhat more accurate values in the reduced transition probabilities given in Table IV we see that only the 238.98- and 439.42-keV states have large  $B(E2)$  values and therefore a highly collective character. As it was pointed out by Robinson *et al.*<sup>3</sup> these two states are an example of the simple weak-coupling model proposed by de-Shalit<sup>9</sup> according to which the  $\frac{1}{2}^-$  single-particle ground state is coupled to the  $2^+$  first excited state of the core to give the two states with spins of  $\frac{3}{2}^-$  and  $\frac{5}{2}^-$ . Thus the  $\frac{3}{2}^- \rightarrow \frac{1}{2}^-$  238.98-keV transition, which is forbidden according to the model,<sup>9</sup> is observed with a  $B(M1)$  value of  $0.095 \pm 0.033$  W.u., while the  $\frac{5}{2}^- \rightarrow \frac{3}{2}^-$  200.40-keV transition between the two members of the doublet has a  $B(M1)$  value of  $0.053 \pm 0.004$  W.u.. In the weak-coupling model<sup>9</sup> from the  $B(M1)$  value for the  $\frac{5}{2}^- \rightarrow \frac{3}{2}^-$  200.40-keV transition we obtain the value of  $(g_c - g_p)^2 = 1.006 \pm 0.064$  by employing the present results and the quantities summarized in Table IV. By assuming the ground-state value  $g_p = 1.068 \mu_N$  we obtain  $g_c = (0.065 \pm 0.064)$  or  $(2.071 \pm 0.064) \mu_N$ . We further note that the  $\Delta I$ -forbidden 277.47-keV transition between the 439.42- and 161.83-keV levels in the weak-coupling model<sup>9</sup> is found to be retarded by  $(1.1 \pm 0.1) \times 10^5$  over the Weisskopf

TABLE IV. Summary of the deduced multipole mixing ratios for transitions in  $^{77}\text{Se}$ .

$E$ level (keV)	$\tau$	Transition (keV)		$J_i^\pi \rightarrow J_f^\pi$	$\delta(E2/M1)$	$B(E2)$ values	$B(M1)$ values
239.0	$(24 \pm 8)^a$ psec	(3 $\rightarrow$ 0)	239.0	$\frac{3}{2}^- \rightarrow \frac{1}{2}^-$	$0.13 \pm 4$	$45 \pm 4$	$0.095 \pm 0.033$
249.65	$(13.5 \pm 0.5)$ nsec	(4 $\rightarrow$ 0)	249.8	$\frac{5}{2}^- \rightarrow \frac{1}{2}^-$	$E2$	$2.1 \pm 0.1$	$(2.6 \pm 0.1) \times 10^{-5}$ <sup>c</sup>
		(4 $\rightarrow$ 1)	87.6	$\frac{5}{2}^- \rightarrow \frac{1}{2}^+$	$-0.09 \pm 5^b$		
439.4	$(31.7 \pm 2.0)$ psec	(6 $\rightarrow$ 0)	439.5	$\frac{5}{2}^- \rightarrow \frac{1}{2}^-$	$E2$	$45 \pm 3$	$(9.1 \pm 0.9) \times 10^{-6}$ <sup>c</sup>
		(6 $\rightarrow$ 1)	277.5	$\frac{5}{2}^- \rightarrow \frac{3}{2}^+$	$E1$		
		(6 $\rightarrow$ 3)	200.4	$\frac{5}{2}^- \rightarrow \frac{3}{2}^-$	$0.0 \pm 1$	$\leq 18$	
520.6	$(10^{+\frac{8}{-8}})^d$ psec	(7 $\rightarrow$ 0)	520.6	$\frac{3}{2}^- \rightarrow \frac{1}{2}^-$	$0.17^{+\frac{8}{-1}}$ or $1.2 \pm 2$	$2.8^{+4.4}_{-1.2}$	$0.020^{+0.031}_{-0.008}$
		(7 $\rightarrow$ 3)	281.7	$\frac{3}{2}^- \rightarrow \frac{3}{2}^-$	$-0.12^{+\frac{3}{-4}}$	$3.1^{+4.8}_{-1.2}$	$0.013^{+0.020}_{-0.005}$
		(7 $\rightarrow$ 4)	270.8	$\frac{3}{2}^- \rightarrow \frac{5}{2}^-$	$0.30^{+\frac{5}{-6}}$	$3.1^{+4.7}_{-1.1}$	$0.0019^{+0.0030}_{-0.0008}$
817.8		(10 $\rightarrow$ 0)	817.8	$\frac{1}{2}^- \rightarrow \frac{1}{2}^-$	Pure $M1$		
		(10 $\rightarrow$ 3)	578.7	$\frac{1}{2}^- \rightarrow \frac{3}{2}^-$	$0.16^{+\frac{3}{-4}}$ or $-2.6^{+\frac{2}{-2}}$		
		(10 $\rightarrow$ 4)	567.9	$\frac{1}{2}^- \rightarrow \frac{5}{2}^-$	$E2$		
		(10 $\rightarrow$ 6)	378.5	$\frac{1}{2}^- \rightarrow \frac{5}{2}^-$	$E2$		
		(10 $\rightarrow$ 7)	297.2	$\frac{1}{2}^- \rightarrow \frac{3}{2}^-$	$0.17 \pm 3$ or $-2.7 \pm 2$		
824.4		(11 $\rightarrow$ 0)	824.4	$\frac{5}{2}^- \rightarrow \frac{1}{2}^-$	$E2$		
		(11 $\rightarrow$ 4)	574.6	if $\frac{3}{2}^- \rightarrow \frac{5}{2}^-$	$0.23 \pm 6$		
				if $\frac{5}{2}^- \rightarrow \frac{5}{2}^-$	$-0.33^{+\frac{8}{-9}}$		
		(11 $\rightarrow$ 7)	303.8	if $\frac{3}{2}^- \rightarrow \frac{3}{2}^-$	$-0.44^{+\frac{5}{-16}}$ or $-6.3^{+\frac{26}{-51}}$		
				if $\frac{5}{2}^- \rightarrow \frac{3}{2}^-$	$0.09^{+\frac{5}{-4}}$ or $-8.1^{+\frac{18}{-33}}$		
		(11 $\rightarrow$ 6)	385.0	if $\frac{5}{2}^- \rightarrow \frac{5}{2}^-$	$-0.23^{+\frac{7}{-5}}$		
		(11 $\rightarrow$ 8)	243.6	if $\frac{3}{2}^- \rightarrow \frac{5}{2}^-$	$0.31 \pm 5$		
$(\frac{3}{2}^-, \frac{5}{2}^-) \rightarrow \frac{5}{2}^+$	$E1$						
(11 $\rightarrow$ 9)	144.5	$(\frac{3}{2}^-, \frac{5}{2}^-) \rightarrow \frac{5}{2}^+$	$E1$				
1005.1		(13 $\rightarrow$ 4)	755.4	$\frac{3}{2}^- \rightarrow \frac{5}{2}^-$	$-0.31^{+\frac{9}{-8}}$		
		(13 $\rightarrow$ 5)	704.1	$\frac{3}{2}^- \rightarrow \frac{5}{2}^+$	$E1$		
		(13 $\rightarrow$ 7)	484.6	$\frac{3}{2}^- \rightarrow \frac{3}{2}^-$	$-0.27^{+\frac{4}{-3}}$		
		(13 $\rightarrow$ 8)	424.1	$\frac{3}{2}^- \rightarrow \frac{5}{2}^+$	$E1$		

<sup>a</sup> Value deduced from the  $B(E2)$  of Ref. 3 given in column 6, using the  $\delta$  value of 0.13 from this work.<sup>b</sup> Value for the mixing ratio  $\delta(M2/E1)$ .<sup>c</sup> Value for  $B(E1)$  in W.u.<sup>d</sup> Weighted average from Refs. 3, 6, and 20-25.

estimated.

The level structure of  $^{77}\text{Se}$  has been discussed on the basis of several models without substantial success. For example, Engels<sup>12</sup> proposes that the Nilsson model for the deformed nuclei is applicable here. In particular the 238.98- ( $\frac{3}{2}^-$ ) and 439.42-keV ( $\frac{5}{2}^-$ ) levels were considered as members of a  $K = \frac{1}{2}$  band built on the  $\frac{1}{2}^-$  ground state. Furthermore the 808-keV level in  $^{77}\text{Se}$  was considered as a possible candidate for the  $\frac{7}{2}^-$  member of this band by Rabenstein and Vonach.<sup>4</sup> Evidence for any other bands on other Nilsson single-particle states in  $^{77}\text{Se}$  is not available at the present time. It is quite evident that such a description would be justified only when the higher-spin members of such bands are definitely identified.

The structure of nuclei such as  $^{99,101}\text{Rh}$ ,  $^{95,97}\text{Tc}$ , etc., similar to  $^{77}\text{Se}$  in which the protons rather than the neutrons are filling the  $g_{9/2}$  orbit has been discussed<sup>29-32</sup> in terms of the pairing-plus-quadrupole model and various extensions of it. Particular difficulty is encountered in explaining the nature of the low-lying  $\frac{5}{2}^+$  and  $\frac{7}{2}^+$  states.

Further comprehensive theoretical calculations are required to satisfactorily explain the structure of the  $g_{9/2}$  nuclei. A search for low-lying high-spin states in  $^{77}\text{Se}$  with lifetime measurements via in-beam reaction spectrometry when combined with the present  $\delta(E2/M1)$  values will provide the necessary information that would establish the most appropriate theoretical description for this nucleus.

---

\*Work supported in part by the U.S. Atomic Energy Commission under Contracts Nos. AT(11-1)-1530 and AT(11-1)-1760.

<sup>1</sup>B. E. F. Macefield, R. Middleton, and D. J. Pullen, *Nucl. Phys.* **44**, 309 (1963).

<sup>2</sup>E. K. Lin, *Phys. Rev.* **139**, B340 (1965).

<sup>3</sup>R. L. Robinson, F. K. McGowan, and P. H. Stelson, *Phys. Rev.* **125**, 1373 (1962); R. L. Robinson, P. H. Stelson, F. K. McGowan, J. L. C. Ford, Jr., and W. T. Milner, *Nucl. Phys.* **74**, 281 (1965).

<sup>4</sup>D. Rabenstein and H. Vonach, *Z. Naturforsch.* **26a**, 458 (1971).

<sup>5</sup>R. Knerr and H. Vonach, *Z. Phys.* **246**, 151 (1971).

<sup>6</sup>S. Monaro, *Nuovo Cimento* **30**, 1379 (1963).

<sup>7</sup>G. Ardisson and C. Ythier, *Physica* **34**, 53 (1967).

<sup>8</sup>D. G. Sarantites and B. R. Erdal, *Phys. Rev.* **177**, 1631 (1969).

<sup>9</sup>A. de-Shalit, *Phys. Rev.* **122**, 1530 (1961).

<sup>10</sup>L. S. Kisslinger and R. A. Sorensen, *Rev. Mod. Phys.* **35**, 853 (1963).

<sup>11</sup>O. Nathan and S. G. Nilsson, in *Alpha-, Beta-, and Gamma-Ray Spectroscopy*, edited by K. Siegbahn (North-Holland, Amsterdam, 1965), Chap. X.

<sup>12</sup>W. Engels, *Z. Naturforsch.* **22a**, 2004 (1967).

<sup>13</sup>H. Ikegami and M. Sano, *Phys. Lett.* **21**, 323 (1966).

<sup>14</sup>A. Goswami, D. K. McDaniels, and O. Nalcioglu, *Phys. Rev. C* **7**, 1263 (1973).

<sup>15</sup>M. E. Phelps, D. G. Sarantites, and W. G. Winn, *Nucl. Phys.* **A149**, 647 (1970).

<sup>16</sup>W. G. Winn and D. G. Sarantites, *Nucl. Instrum. Methods* **66**, 61 (1968); **82**, 230 (1970).

<sup>17</sup>D. C. Camp and A. L. Van Lehn, *Nucl. Instrum.*

*Methods* **76**, 193 (1969).

<sup>18</sup>H. Houtermans, International Atomic Energy Agency, Vienna, private communication.

<sup>19</sup>R. S. Hager and E. C. Seltzer, *Nucl. Data* **A4**, 1 (1968).

<sup>20</sup>N. B. Gove and M. J. Martin, *Nucl. Data* **A10**, 205 (1971).

<sup>21</sup>N. B. Gove and A. H. Wapstra, *Nucl. Data* **A11**, 127 (1972).

<sup>22</sup>H. J. Rose and D. M. Brink, *Rev. Mod. Phys.* **39**, 306 (1967).

<sup>23</sup>W. Engels, W. Deland, U. Wehmann, and E. Bodenstedt, *Phys. Lett.* **11**, 57 (1964).

<sup>24</sup>P. P. Urone, L. L. Lee, Jr., and S. Raman, *Nucl. Data* **B9**, 229 (1973).

<sup>25</sup>R. E. Holland and F. J. Lynch, *Phys. Rev.* **121**, 1464 (1961).

<sup>26</sup>F. J. Lynch and E. N. Shipley, Argonne National Laboratory Report No. ANL-6679, 1963 (unpublished), p. 5.

<sup>27</sup>D. S. Andreev, L. N. Galperin, A. Z. Ilyasov, I. Kh. Lemberg, and I. N. Chugnov, *Izv. Akad. Nauk SSSR Ser. Fiz.* **32**, 226 (1968) [transl.: *Bull. Acad. Sci. USSR Phys. Ser.* **32**, 205 (1968)].

<sup>28</sup>D. G. Sarantites, J. H. Barker, N.-H. Lu, E. J. Hoffman, and D. M. Van Patter, *Phys. Rev. C* **8**, 629 (1973).

<sup>29</sup>M. E. Phelps and D. G. Sarantites, *Nucl. Phys.* **A135**, 116 (1969).

<sup>30</sup>M. E. Phelps and D. G. Sarantites, *Nucl. Phys.* **A159**, 113 (1970).

<sup>31</sup>M. E. Phelps and D. G. Sarantites, *Nucl. Phys.* **A171**, 44 (1971).

<sup>32</sup>A. C. Xenoulis and D. G. Sarantites, *Phys. Rev. C* **7**, 1193 (1973).